0026-895X/02/6205-1187–1197
MOLECULAR PHARMACOLOGY
U.S. Government work not protected by U.S. copyright
Mol Pharmacol 62:1187–1197, 2002

Vol. 62, No. 5
1942/1011161
Printed in U.S.A.

Purinergic $P2X_2$ Receptor Desensitization Depends on Coupling between Ectodomain and C-Terminal Domain

MU-LAN HE, TAKA-AKI KOSHIMIZU,[1] MELANIJA TOMIĆ, and STANKO S. STOJILKOVIC

Endocrinology and Reproduction Research Branch, National Institute of Child Health and Human Development, National Institutes of Health, Bethesda, Maryland

Received June 19, 2002; accepted August 14, 2002

This article is available online at http://molpharm.aspetjournals.org

ABSTRACT

The wild-type $P2X_2$ purinergic receptor ($P2X_{2a}R$) and its splice form lacking the intracellular Val^{370}-Gln^{438} C-terminal sequence ($P2X_{2b}R$) respond to ATP stimulation with comparable EC_{50} values and peak current/calcium responses but desensitize in a receptor-specific manner. $P2X_{2a}R$ desensitizes slowly and $P2X_{2b}R$ desensitizes rapidly. We studied the effects of different agonists, and of substituting the ectodomain, on the pattern of calcium signaling by $P2X_{2a}R$ and $P2X_{2b}R$. Both receptors showed similar EC_{50} values (estimated from the peak calcium response) and IC_{50} values (estimated from the rate of calcium signal desensitization) for agonists, in the order 2-MeS-ATP $\leq$ ATP $\leq$ ATPγS $<$ BzATP $\ll$ $\alpha\beta$-meATP, and the IC_{50} values for agonists were shifted to the right compared with their EC_{50} values. Furthermore, the ATP-induced receptor-subtype specific pattern of desensitization was mimicked by high- but not by low-efficacy agonists, suggesting a ligand-specific desensitization pattern. To test this hypothesis, we generated chimeric $P2X_{2a}R$ and $P2X_{2b}R$ containing the Val^{60}-Phe^{301} ectodomain sequence of $P2X_3R$ and Val^{61}-Phe^{313} ectodomain sequence of $P2X_7R$ instead the native Ile^{66}-Tyr^{310} sequence. The mutated $P2X_{2a}+X_3R$ and $P2X_{2b}+X_3R$ exhibited comparable EC_{50} values for ATP, BzATP, and $\alpha\beta$-meATP in the submicromolar concentration range and desensitized in a receptor-specific and ligand-nonspecific manner. On the other hand, the chimeric $P2X_2+X_7R$ exhibited decreased sensitivity for ATP and desensitized in a receptor-nonspecific manner. These results suggest that efficacy of agonists for the ligand-binding domain of $P2X_2$Rs reflects the strength of desensitization controlled by their C-terminal structures.

During the prolonged agonist occupancy, ATP-gated purinergic receptor-channels (P2XRs) become refractory to the stimulus and cellular responses decline. This process, called desensitization, is common for ligand-gated channels and occurs because liganded receptors enter stable conformations through which ion permeation is blocked or attenuated. Based on the observed differences in their desensitization kinetics, homomeric P2XRs are generally divided into three groups: $P2X_1R$ and $P2X_3R$ desensitize very rapidly and $P2X_4R$ and $P2X_6R$ desensitize with a moderate rate, whereas $P2X_2R$, $P2X_5R$, and $P2X_7R$ show little or no desensitization (North and Barnard, 1997; Ralevic and Burnstock, 1998). Heteromultimerization results in channels that desensitize with different kinetics from those seen in cells expressing homomeric channels; the influence of participating subunits on channel desensitization pattern is well documented for $P2X_2R+P2X_3R$ (Lewis et al., 1995; Radford et al., 1997). The differences in desensitization rates of P2XRs are reminiscent of those seen among subtypes of other ligand-gated receptor-channels (McBain and Mayer, 1994; Lerma et al., 2001).

The underlying molecular mechanisms of P2XR desensitization have been incompletely characterized. Calcium and other divalent cations influence the rate of desensitization and the rate of recovery from desensitization in native and cloned channels (Cook et al., 1998; Ding and Sachs, 2000). A highly conserved protein kinase C site located in the N terminus of P2XRs may control the rate of desensitization of $P2X_1R$, $P2X_2R$, and $P2X_3R$ (Boue-Grabot et al., 2000; Paukert et al., 2001; Ennion and Evans, 2002). Phosphorylation of a protein kinase A site in the C terminus of $P2X_{2a}R$ may also participate in receptor desensitization (Chow and Wang, 1998). Experiments with chimeras composed of $P2X_2R$ and $P2X_1R$ or $P2X_3R$ subunits suggested that the rapid desensitization requires interactions between two transmembrane domains of receptor subunits (Werner et al., 1996). Several groups have also reported that the C-terminal splice variant of $P2X_2R$, called $P2X_{2b}R$ or $P2X_{2-2}R$, lacks a stretch of 69 residues and desensitizes faster than the full-length channel, called $P2X_{2a}R$ (Brandle et al., 1997; Simon et al., 1997; Ko-

[1] Current address: Department of Molecular Cell Pharmacology, National Children's Medical Research Center, Tokyo, Japan.

ABBREVIATIONS: P2X, purinergic receptor channels; PCR, polymerase chain reaction; EGFP, enhanced green fluorescent protein; GFP, green fluorescent protein; 2-MeS-ATP, 2-methylthio-ATP; ATPγS, adenosine-5′-*O*-(3-thiotriphosphate); BzATP, 3′-*O*-(4-benzoyl)benzoyl-ATP; $\alpha\beta$-meATP, α,β-methylene-ATP; AMPA, α-amino-3-hydroxy-5-methyl-4-isoxazolepropionic acid.

shimizu et al., 1998b). The site-directed mutagenesis experiments suggested important roles of different residues in the C-terminal tail in $P2X_2R$ desensitization (Koshimizu et al., 1998a; Zhou et al., 1998; Smith et al., 1999). The variable C-terminal structures may also influence the desensitization rates of other members of P2XRs, including $P2X_3R$ and $P2X_4R$ (Koshimizu et al., 1999). A large C terminus of $P2X_7R$ also accounts for the nondesensitizing pattern of these channels during repetitive stimulation (Surprenant et al., 1996).

Here, we examined the interactions between the ectodomain and C-terminal domain in controlling the pattern of P2XR desensitization. Specifically, we studied the effects of altering the agonist and substituting the ectodomain on the pattern of calcium signaling by P2XRs. For this purpose, we used $P2X_{2a}R$ and $P2X_{2b}R$ because of their identical ectodomains and distinct desensitization patterns in response to ATP. The $P2X_2$ receptor-subtype specific desensitization pattern was observed not only in current measurements, but also in single-cell calcium measurements (Koshimizu et al., 1998, 2000), indicating that such recordings are sufficient for studies with this particular receptor. These experiments revealed that the structure-dependent desensitization pattern of $P2X_{2a}R$ and $P2X_{2b}R$ reflects the efficacy of agonists for these receptors.

Materials and Methods

DNA Constructs. The coding sequences of the rat $P2X_{2a}$, $P2X_{2b}$, $P2X_3$, and $P2X_7$ subunits were isolated by reverse transcription-PCR (Koshimizu et al., 1999), and subcloned into the bicistronic enhanced fluorescent protein expression vector pIRES2-EGFP (BD Clontech, Palo Alto, CA) at the restriction enzyme sits of *Xho*I/*Pst*I for $P2X_{2a}R$ and $P2X_{2b}R$, and *Xho*I/*Eco*RI for $P2X_3R$ and $P2X_7R$. Chimeric subunits, termed $P2X_{2a}+X_3EC$ and $P2X_{2b}+X_3EC$, contain extracellular domain from Val^{60} to Phe^{301} of $P2X_3R$ instead of the native Ile^{66}-Tyr^{310} sequence of $P2X_{2a}R$ and $P2X_{2b}R$ (Fig. 1). To exchange the corresponding extracellular regions, two restriction endonuclease sites for *Sac*I and *Eco*RI were introduced into both $P2X_2$ and $P2X_3$ subunits using PCR-based overlap extension method (Horton et al., 1989). Primer sequences carrying silent nucleotide substitutions (underlined) are as follows: X2EcoL, 5′-AACATCGATTCGAATTCCATAGGCTTTGAT-3′; X3SacU, 5′-ATTGAGAGCTCAGTAGTTACAAAGGTG-3′; X3SacL, 5′-GCTCTCAATGGCGGTGTCCCTCACTTG-3′; X3EcoU, 5′-GGAATTCGCTTTGATGTGCTGGTA-3′; and X3EcoL, 5′-GCGAATTCCAAAAGCCTTCAGGAGTGT-3′. By two rounds of PCR, the entire protein coding regions for the *Sac*I/*Eco*RI-carrying $P2X_{2a}$, $P2X_{2b}$, and $P2X_3$ subunits, termed $P2X_{2a}$SE, $P2X_{2b}$SE, and $P2X_3$SE, were amplified as described previously (Koshimizu et al., 1999). Before subcloning these PCR products, pBluescript vector (Stratagene, La Jolla, CA) was digested with *Sac*I, treated with Klenow enzyme for end-filling, and self-ligated to remove this intrinsic *Sac*I site. The PCR products were then subcloned into *Hinc*II/*Sma*I site of the modified pBluescript vector and sequenced. Correctly subcloned inserts were digested with *Sac*I and *Eco*RI and the fragment corresponding to the putative extracellular loop of $P2X_3R$ was transferred to $P2X_{2a}$SE and $P2X_{2b}$SE, generating chimeric receptors, $P2X_{2a}+X_3EC$ and $P2X_{2b}+X_3EC$, respectively. For mammalian expression, the *Nhe*I/*Xho*I digested fragments of $P2X_{2a}+X_3EC$ and $P2X_{2b}+X_3EC$ were also transferred to pIRES2-EGFP.

$P2X_{2a}+X_7EC$ and $P2X_{2b}+X_7EC$ were directly constructed by overlap extension PCR using the corresponding wild-type P2XRs cDNA as templates (Fig. 1). Mutagenesis primers were pairs of chimeric sense and antisense that were 36-mer long, with the joint sites positioned in the center. The constructed $P2X_{2a}+X_7EC$ and $P2X_{2b}+X_7EC$ chimeric subunits contain Val^{61}-Phe^{313} extracellular domain of $P2X_7R$ instead the native sequence Ile^{66}-Tyr^{310}. These chimeric P2XRs were also subcloned into GFP-expression vector pIRES2-EGFP. The identity of all constructs was verified by BigDye Terminator cycle sequencing (Applied Biosystems, Foster City, CA) performed by Laboratory of Molecular Technology (National Cancer Institute, Frederick, MD). Large-scale plasmid DNA for transfection was prepared by using the Plasmid Maxi Kit (QIAGEN Co., GmbH, Germany).

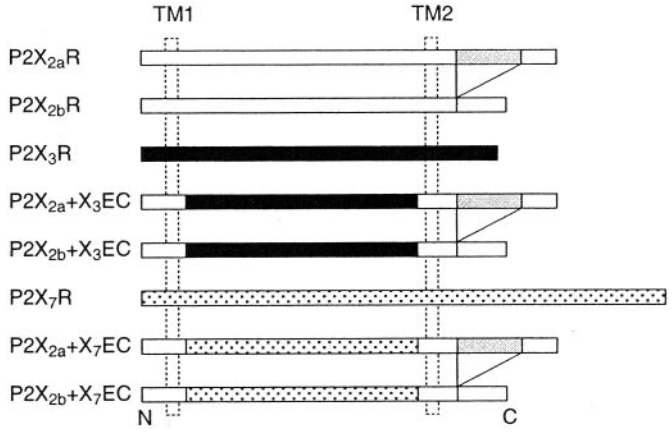

Fig. 1. Schematic representation of the wild-type and chimeric constructs used in this study. White horizontal rectangles indicate $P2X_{2a}R$ and its spliced form lacking the Val^{370}-Gln^{438} C-terminal sequence (shown in gray), called $P2X_{2b}R$, black rectangles indicate $P2X_3R$, and dotted rectangles indicate $P2X_7R$. Vertical dashed rectangles indicate the positions of putative transmembrane domains TM1 and TM2. The constructed $P2X_{2a}+X_3EC$ and $P2X_{2b}+X_3EC$ chimeric receptors contain Val^{60}-Phe^{301} extracellular domain sequence of $P2X_3R$ instead the native Ile^{66}-Tyr^{310} sequence of $P2X_{2a}R$ and $P2X_{2b}R$. The constructed $P2X_{2a}+X_7EC$ and $P2X_{2b}+X_7EC$ chimeric subunits contain Val^{61}-Phe^{313} extracellular domain of $P2X_7R$ instead the native sequence Ile^{66}-Tyr^{310}.

Cell Culture and Transient Transfection. Mouse immortalized gonadotropin-releasing hormone-secreting GT1–7 cells (GT1 cells) were used to examine the patterns of Ca^{2+} signaling evoked by P2XRs as described previously (Koshimizu et al., 1999). GT1 cells were routinely maintained in Dulbecco's modified Eagle's medium/Ham's F12 medium (1:1), containing 10% (v/v) fetal bovine serum and 100 μg/ml gentamicin (Invitrogen Corp., Carlsbad, CA) in a water-saturated atmosphere of 5% CO_2 and 95% air at 37°C. Before the day of transfection, cells were plated on 25-mm coverslips coated with poly(L-lysine) (0.01% w/v; Sigma, St. Louis, MO) at a density of $0.75–1.0 \times 10^5$ cells per 35-mm dish. For each dish of cells, transient transfection of expression constructs was conducted using 1 μg of DNA and 7 μl of LipofectAMINE 2000 Reagent (Invitrogen) in 3 ml of serum-free Opti-MEM. After 6 h of incubation, transfection mixture was replaced with normal culture medium. Cells were subjected to experiments 24 to 48 h after transfection.

$[Ca^{2+}]_i$ Measurements. Transfected GT1 cells were preloaded with 1 μM Fura-2 acetoxymethyl ester (Molecular Probes, Eugene, OR) for 60 min at room temperature in modified Kreb's Ringer buffer (120 mM NaCl, 5 mM KCl, 1.2 mM $CaCl_2$, 1.2 mM KH_2PO_4, 0.7 mM $MgSO_4$, 1.8 g/l Glucose, and 15 mM HEPES, pH 7.4). After dye loading, cells were incubated in modified Kreb's Ringer buffer and kept in the dark for at least 30 min before single-cell $[Ca^{2+}]_i$ measurement. Coverslips with cells were mounted on the stage of an Axiovert 135 microscope (Carl Zeiss, Oberkochen, Germany) attached to the Attofluor Digital Fluorescence Microscopy System (Atto Instruments, Rockville, MD). Cells were stimulated with various doses of agonists (added by pipette at room temperature) and the dynamic changes of $[Ca^{2+}]_i$ were examined under a 40× oil-immersion objective during exposure to alternating 340 and 380 nm light beams, and the intensity of light emission at 520 nm was measured. The ratio of light intensities, F_{340}/F_{380}, that reflects changes in $[Ca^{2+}]_i$ was simultaneously followed in several single

cells. Apyrase (Grade I; Sigma, St. Louis, MO) was used at 0.2 U/ml throughout the incubation process, loading with Fura-2 acetoxymethyl ester, and $[Ca^{2+}]_i$ recording in cells expressing $P2X_3R$, $P2X_{2a}+X_3EC$, and $P2X_{2b}+X_3EC$ receptors. Experiments with $P2X_{2a}R$, $P2X_{2b}R$, $P2X_7R$, and their chimeras were done without apyrase. GFP was used as a marker for cells with P2XR expression as described previously (Koshimizu et al., 1999, 2000). Cells expressing GFP were optically detected by an emission signal at 520 nm when excited by 488-nm ultraviolet light and were not detectable by 340- and 380-nm excitations in the absence of Fura-2.

Calculations. To minimize the impact of receptor saturation kinetics on the $[Ca^{2+}]_i$ profiles, agonists were added rapidly and were continuously present during the recording. Thus, the rise in $[Ca^{2+}]_i$ predominantly reflects the bound-open equilibrium, whereas the decay represents the equilibration into desensitization state (Auerbach and Akk, 1998). The time course of the $[Ca^{2+}]_i$ was fitted to a single exponential function using Prism software (GraphPad Software, San Diego, CA). All values in the text are reported as mean ± S.E.M. Significant differences, with $P < 0.05$, were determined by one-way analysis of variance with Newman-Keuls multiple comparison test. Concentration-response relationships were fitted to a four-parameter logistic equation using a nonlinear curve-fitting program (Kaleidagraph; Synergy Software, Reading, PA) that derives the EC_{50} and Hill values. Calcium recordings were done in 15 to 50 cells simultaneously, and each experiment was repeated three or more times to ensure the reproducibility of the findings.

Results

$P2X_{2a}R$ and $P2X_{2b}R$ Exhibit Similar EC_{50} Values for Agonists. The native and chimeric P2XRs were subcloned into GFP-expression vector pIRES2-EGFP, and the relative transfection efficiency of P2XRs constructs was estimated in single cells by analyzing the intensity of fluorescence signals, as described previously (Koshimizu et al., 2000). In the presence of fixed amount of expression constructs and comparable post-transfection times, the percentage of GFP+ATP-positive cells varied between 45 and 60% and was independent on the channel type expressed. When the average GFP fluorescence was similar for each set of cells (about 60 arbitrary units), the mean amplitude of peak $[Ca^{2+}]_i$ to 100 μM ATP were highly reproducible for the same channel types. No repetitive stimulation was done to avoid the possible impact of desensitization on the amplitude and pattern of $[Ca^{2+}]_i$ signals. Also, in all experiments agonists were added rapidly to the coverslip dish to minimize the impact of agonist diffusion on the profile of $[Ca^{2+}]_i$ signals.

Under these experimental conditions, $P2X_{2a}R$ and $P2X_{2b}R$ responded to ATP stimulation, as well as to 2-MeS-ATP, ATPγS, BzATP, and $\alpha\beta$-meATP stimulation, with a rapid rise in $[Ca^{2+}]_i$, followed by a gradual decline to the steady plateau levels. Figure 2 shows typical patterns of $[Ca^{2+}]_i$

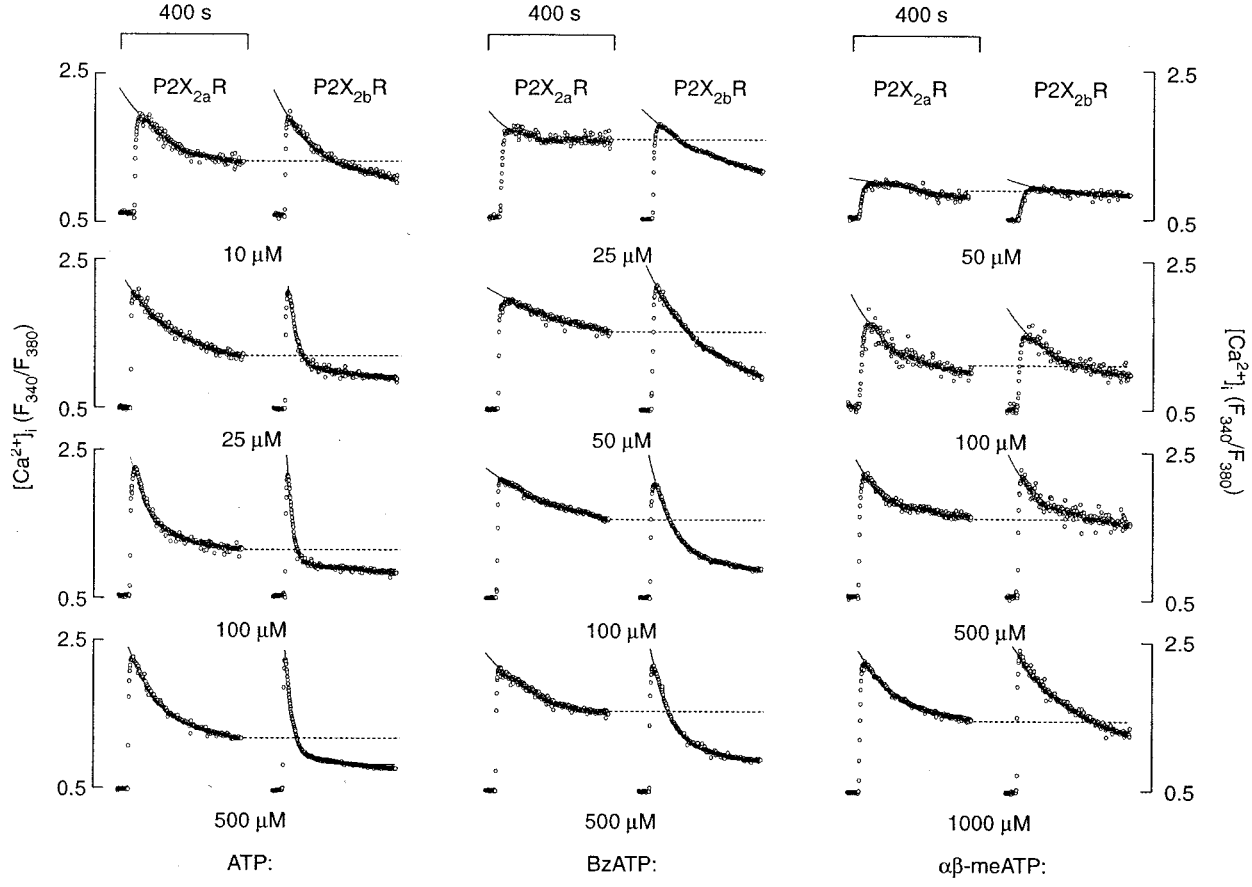

Fig. 2. Comparison of the effects of ATP and two analogs, BzATP and α,β-meATP, on the peak calcium response and rates of signal desensitization in cells expressing $P2X_{2a}R$ and $P2X_{2b}R$. In this and following figures, experimental records are shown by open circles (mean values from at least 15 traces in representative experiments) and fitted curves by full lines. A single exponential function was sufficient to describe the desensitization rates. The fitted function is extrapolated for clarity. Agonists were added in concentrations indicated below traces and were continuously present during the recording.

signals in response to stimulation with increasing ATP (left), BzATP (middle), and $\alpha\beta$-meATP (right) concentrations. At high agonist concentrations, the peak $[Ca^{2+}]_i$ responses induced by ATP, BzATP, and $\alpha\beta$-meATP (Fig. 2), as well as by 2-MeS-ATP and ATPγS (data not shown), were comparable. Figure 3 illustrates the sigmoidal concentration-dependence of ATP, BzATP, and $\alpha\beta$-meATP on the amplitude of $[Ca^{2+}]_i$ responses, shown as the mean values of peak response minus baseline. The dotted lines and numbers above the lines illustrate the EC_{50} values for these agonists. The calculated EC_{50} values for 2-MeS-ATP were slightly lower and for ATPγS slightly higher compared with ATP. Thus, both receptors show similar EC_{50} values for agonists, in the order: 2-MeS-ATP $\leq$ ATP $\leq$ ATPγS $\leq$ BzATP $\ll$ $\alpha\beta$-meATP.

The C-Terminal-Dependent Desensitization Pattern of $P2X_2R$ Is Ligand-Specific. The desensitization rates of $[Ca^{2+}]_i$ signals generated by two receptors were also dependent on agonist concentrations. Figure 2, left, shows typical desensitization profiles in $P2X_{2a}R$- and $P2X_{2b}R$-expressing cells stimulated with increasing ATP concentrations. Consistent with the relevance of C-terminal domain structure of $P2X_2Rs$ in control of receptor desensitization (Brandle et al., 1997; Simon et al., 1997; Koshimizu et al., 1998b), $P2X_{2b}R$ desensitized more rapidly than $P2X_{2a}R$ (Fig. 2, left). Stimulation with increasing BzATP and $\alpha\beta$-meATP concentrations also produced a progressive increase in the rates of signal desensitization (Fig. 2, middle and right). Furthermore, $P2X_{2b}R$-expressing cells desensitized more rapidly than $P2X_{2a}R$-expressing cells during the prolonged stimulation with high concentrations of BzATP, whereas signals generated by two receptors desensitized with comparable rates in response to $\alpha\beta$-meATP.

The ligand- and receptor-specificity of signal desensitization is summarized in Fig. 4. The calculated order of agonist concentrations that induce half-maximum rate of signal desensitization (IC_{50} values) was 2-MeS-ATP $\leq$ ATP $\leq$ ATPγS $<$ BzATP $\ll$ $\alpha\beta$-meATP, and was identical to the EC_{50} values order. However, the IC_{50} values for agonists were shifted to the right compared with EC_{50} values. For example, the EC_{50} values for ATP were 2 and 3 μM for $P2X_{2a}R$ and $P2X_{2b}R$ (Fig. 3), respectively, whereas the IC_{50} values for the same agonist were 26 and 29 μM, respectively (Fig. 4, A–C). In parallel to the concentration-dependence of peak $[Ca^{2+}]_i$ responses, the rates of $P2X_{2a}R$ desensitization reached comparable levels at saturating ATP, BzATP, and $\alpha\beta$-meATP concentrations (Fig. 4, A–C, dotted line). In contrast to the activation of channels, BzATP was unable to mimic the action of ATP on the rates of $P2X_{2b}R$ desensitization when added in the 1 to 1000 μM concentration range. Furthermore, the receptor subtype-specific pattern of signal desensitization was completely lost in cells stimulated with $\alpha\beta$-meATP, a low potency agonist.

The ligand-specific $P2X_{2b}R$ desensitization pattern was further illustrated in Fig. 4, D–F. When $P2X_{2b}R$-expressing cells were stimulated with high (500 μM) agonist concentrations for a prolonged time, they responded with comparable amplitudes of $[Ca^{2+}]_i$ spikes but with variable rates of signal desensitization (Fig. 4, D and E). There was an inverse relationship between the EC_{50} values for agonists and the rates of receptor desensitization estimated at 500 μM concentrations (Fig. 4F). These data indicate that the C terminus-specific desensitization pattern was affected when low potency agonists were used.

Increase in $P2X_2R$ Sensitivity for Agonists Facilitates Desensitization. We further examined the agonist-specific desensitization pattern of $P2X_2Rs$ by producing the chimeric receptors with increased and decreased sensitivity for agonists. To make $P2X_2Rs$ with high sensitivity for agonists, we constructed chimeric receptors containing the Val^{60}-Phe^{301} extracellular domain sequence of $P2X_3R$ instead the native Ile^{66}-Tyr^{310} sequence, and called them $P2X_{2a}+X_3EC$ and $P2X_{2b}+X_3EC$ chimeras. In our experimental conditions, the native $P2X_3R$ and $P2X_{2a}+X_3EC$ and $P2X_{2b}+X_3EC$ chimeras did not respond to ATP, BzATP, and $\alpha\beta$-meATP or responded with irregular $[Ca^{2+}]_i$ patterns when cells were incubated without apyrase, whereas the pattern of responses was not affected in $P2X_{2a}R$-and $P2X_{2b}R$-expressing cells. These results confirm our earlier findings (Koshimizu et al., 1999) that endogenous ATP secretion is sufficient to desensitize receptors with high potency for ATP. When experiments were done in the presence of apyrase, all three receptors responded to agonist stimulation in a concentration-dependent manner and with the EC_{50} values for ATP, $\alpha\beta$-meATP, and BzATP in a submicromolar concentration range. Figure 5A, left, illustrates the dose-response to ATP in $P2X_{2a}R+X_3EC$-expressing cells. There was a ~30-fold decrease in EC_{50} for ATP, a ~25-fold decrease for BzATP, and a ~150-fold decrease in EC_{50} for $\alpha\beta$-meATP in $P2X_{2a}R+X_3EC$-expressing cells compared with the native $P2X_{2a}R$ (Fig. 5A). The $P2X_{2b}R+X_3EC$ chimera exhibited the

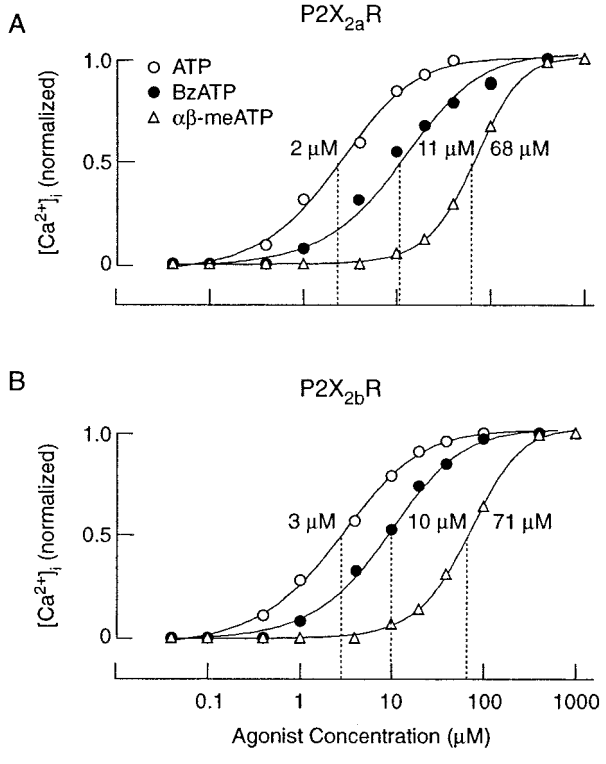

Fig. 3. Concentration dependence of agonist-induced peak calcium response in GT1 neurons expressing homomeric $P2X_{2a}R$ and $P2X_{2b}R$. A and B, comparison of the effects of ATP and its analogs, BzATP and α,β-meATP, on peak calcium response in cells expressing $P2X_{2a}R$ (A) and $P2X_{2b}R$ (B). Data shown are means derived from three to eleven experiments per dose, each done in at least 15 single cells. S.E.M. were within 10%. Numbers above dotted vertical lines indicate the calculated EC_{50} values for three agonists.

same shift in EC_{50} values for two agonists (not shown). On the other hand, the peak amplitude of $[Ca^{2+}]_i$ responses in cells expressing chimeric receptors was 2- to 3-fold higher than that observed in $P2X_3R$-expressing cells (Fig. 5B).

Molecular changes in the ectodomain of $P2X_{2a}R$ and $P2X_{2b}R$ also affected the rates of receptor desensitization. Figure 6, A and B, illustrate typical calcium signal profiles in cells expressing native $P2X_{2a}R$ and $P2X_3R$ and chimeric $P2X_{2a}+X_3EC$ receptors during prolonged stimulation with 100 μM $\alpha\beta$-meATP and 100 μM ATP. Numbers above traces show the mean values for rates of signal desensitization, which are significantly different compared with native $P2X_{2a}R$ and $P2X_3R$. A significant increase in the rates of $P2X_{2a}R+X_3EC$ and $P2X_{2b}R+X_3EC$ desensitization was also observed during stimulation with BzATP. Figure 7 shows typical calcium profiles in $P2X_{2a}R$-, $P2X_{2a}R+X_3EC$-, and $P2X_3R$-expressing cells stimulated with increasing concentrations of BzATP.

In contrast with native $P2X_2Rs$, $P2X_{2a}+X_3EC$ chimera desensitized with comparable rates when stimulated with equimolar ATP, $\alpha\beta$-meATP, and BzATP concentrations (Figs. 6 and 7). $P2X_{2b}+X_3EC$ chimera also desensitized with comparable rates when stimulated with 1 μM ATP, BzATP, and $\alpha\beta$-meATP (Fig. 8). Furthermore, the C terminus-dependent pattern of accelerated desensitization was preserved for ATP stimulation and was developed for $\alpha\beta$-meATP and BzATP stimulation. As shown in Table 1, in all doses studied, there was a significant difference in the rates of $P2X_{2a}+X_3EC$ and $P2X_{2b}+X_3EC$ receptor desensitization. These results support the hypothesis that an increase in the EC_{50} values for agonists introduced by substitution of the extracellular domain results in a loss of ligand-specificity of receptor desensitization.

Decrease in $P2X_2R$ Sensitivity for ATP Blocks C Terminus-Dependent Desensitization. To further test the hypothesis about the relevance of ectodomain for C-terminal structure-dependent desensitization, we made chimeric $P2X_{2a}R$ and $P2X_{2b}R$ with lower sensitivity to ATP and higher sensitivity to BzATP, compared with the wild-type channels. This was achieved by constructing $P2X_{2a}+X_7EC$ and

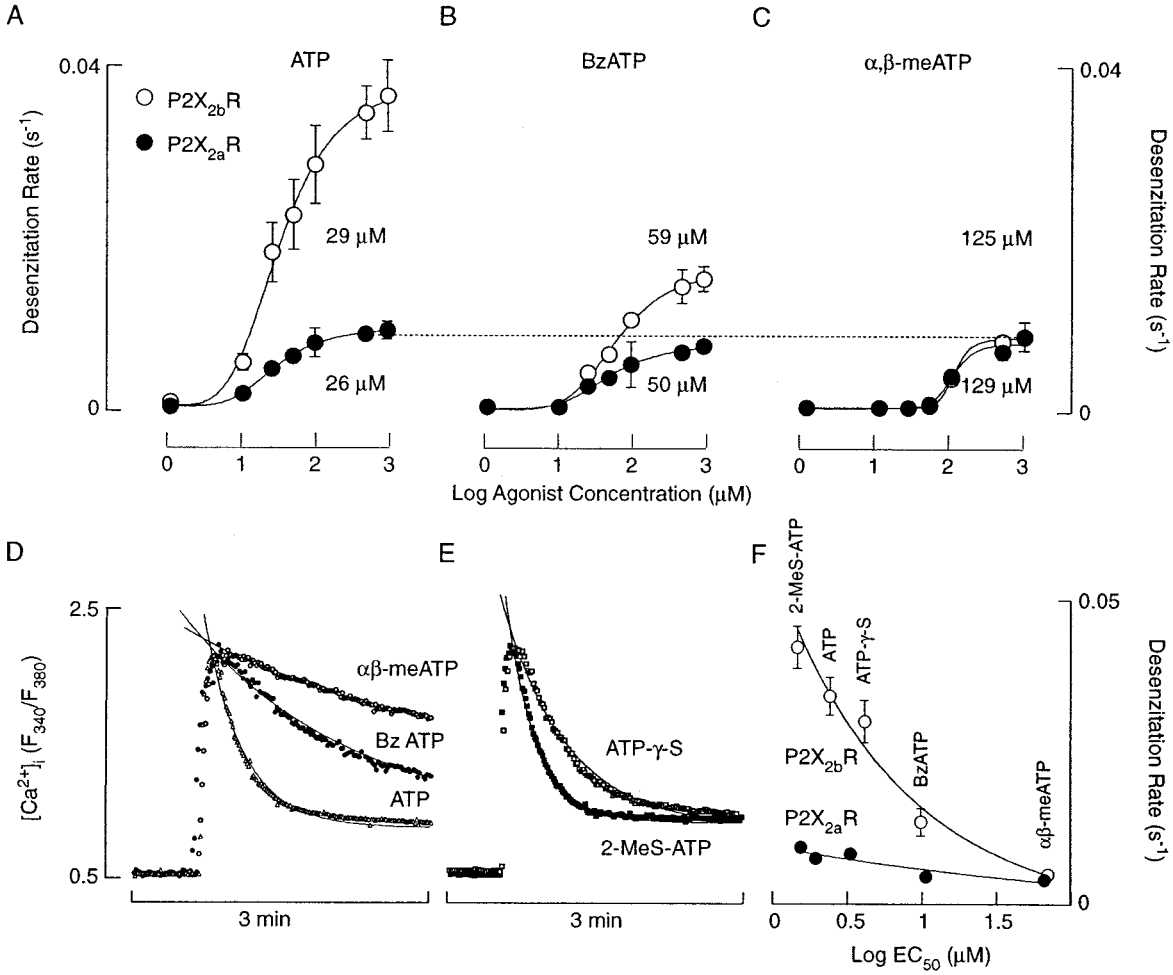

Fig. 4. Ligand-specific receptor desensitization pattern of $P2X_2Rs$. A-C, concentration-dependent effects of agonists on rates of signal desensitization in GT1 neurons expressing homomeric $P2X_{2a}R$ and $P2X_{2b}R$. Circles represent means ± S.E.M. from four to five independent experiments per dose, each performed on 15 to 45 cells. Numbers indicate the calculated IC_{50} values for ATP, BzATP, and $\alpha\beta$-meATP. The dotted horizontal line indicates comparable levels of $P2X_{2a}R$ desensitization rates at high agonist concentrations. To compare IC_{50} values with EC_{50} values, see Fig. 2. D-F, comparison of the effects of 2-MeS-ATP, ATP, ATPγS, BzATP, and $\alpha\beta$-meATP on the rate of $P2X_2Rs$ desensitization. D and E, differences in the rates of calcium signal desensitization in cells expressing $P2X_{2b}R$. Traces shown by open circles are means derived from 15 to 45 cells in a representative experiment. All agonists were added in 500 μM concentrations. F, the relationship between EC_{50} values for agonists and desensitization rates calculated at 500 μM concentrations in $P2X_{2a}R$-and $P2X_{2b}R$-expressing cells.

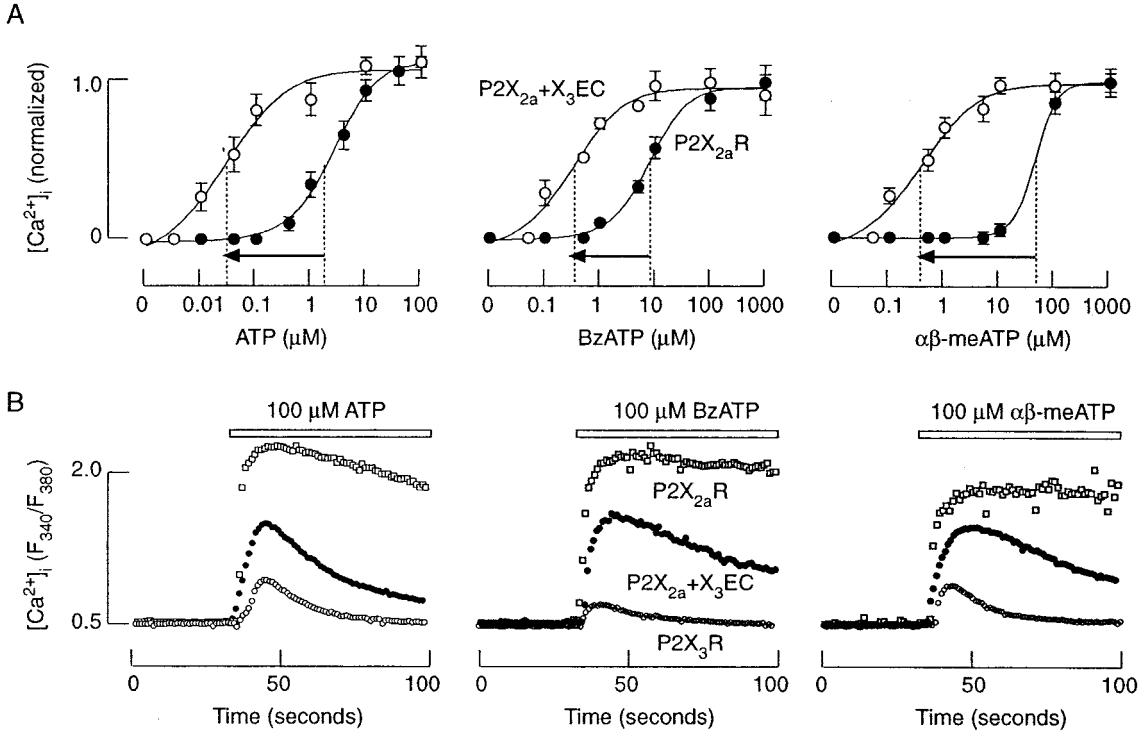

Fig. 5. Influence of the substitution of ectodomain at $P2X_2Rs$ on agonistic potency of ATP (left), BzATP (middle), and $\alpha\beta$-meATP (right). A, change in the EC_{50} values for agonists in cells expressing $P2X_{2a}+X_3EC$ receptor. The results shown are means ± S.E.M. B, comparison of the peak amplitude of $[Ca^{2+}]_i$ signals in $P2X_{2a}+X_3EC$-expressing cells. $P2X_{2b}+X_3EC$ receptors showed comparable leftward shifts in EC_{50} values for three agonists and a decrease in peak amplitude of $[Ca^{2+}]_i$ responses. $P2X_2R+X_3EC$ chimeras were constructed as described under *Materials and Methods*.

$P2X_{2b}+X_7EC$ chimeric receptors containing the Val^{61}-Phe^{313} extracellular domain sequence of $P2X_7R$ instead of the native Ile^{66}-Tyr^{310} sequence. In accordance with the literature (Surprenant et al., 1996), native $P2X_7R$ expressed in GT1 neurons responded to BzATP stimulation with a rapid and non-desensitizing rise in $[Ca^{2+}]_i$ (Fig. 9A), with a calculated EC_{50} of 8 μM (Fig. 9D). In a majority of cells, ATP also induced similar patterns of $[Ca^{2+}]_i$ signaling, albeit of smaller amplitude, whereas a fraction of cells (about 30% in response to 500 and 1000 μM ATP) responded with atypical $[Ca^{2+}]_i$ pro-

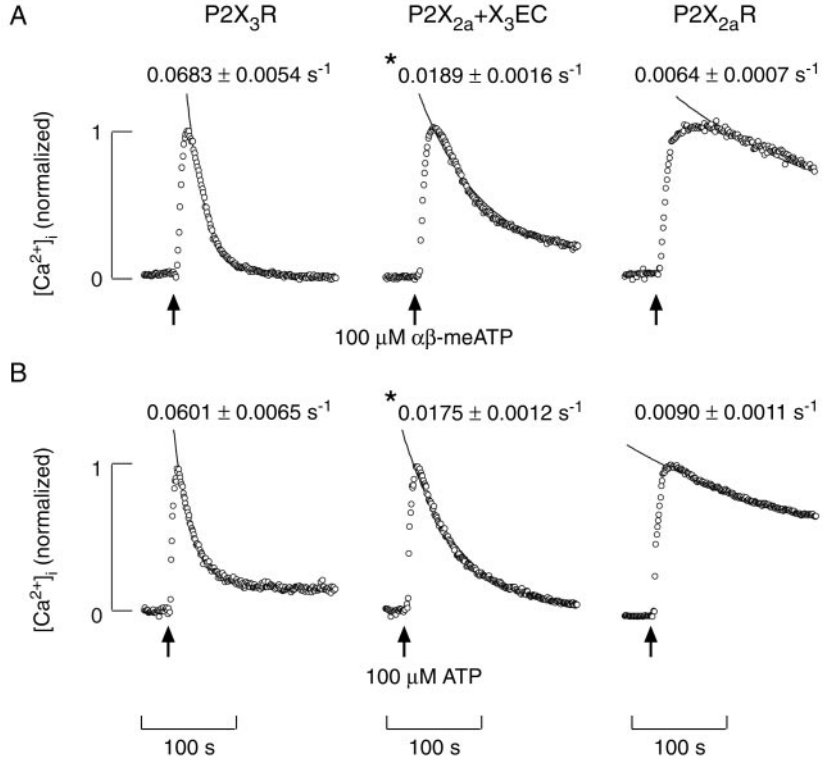

Fig. 6. The pattern of desensitization in cells expressing wild-type $P2X_3R$ and $P2X_{2a}R$ and $P2X_{2a}+X_3EC$ chimera. A and B, comparison of the effects of 100 μM $\alpha\beta$-meATP (A) and 100 μM ATP (B) on the rates of calcium signal desensitization in GT1 neurons expressing $P2X_3R$ (left traces) $P2X_{2a}R+X_3EC$ chimera (central traces), and $P2X_{2a}R$ (right traces). Traces shown are representative from three to eight independent experiments, each done in at least 15 cells. Numbers above traces represent mean ± S.E.M. values of desensitization rates. Asterisks indicate significant differences compared with desensitization rates for $P2X_3R$-and $P2X_{2a}R$-expressing cells.

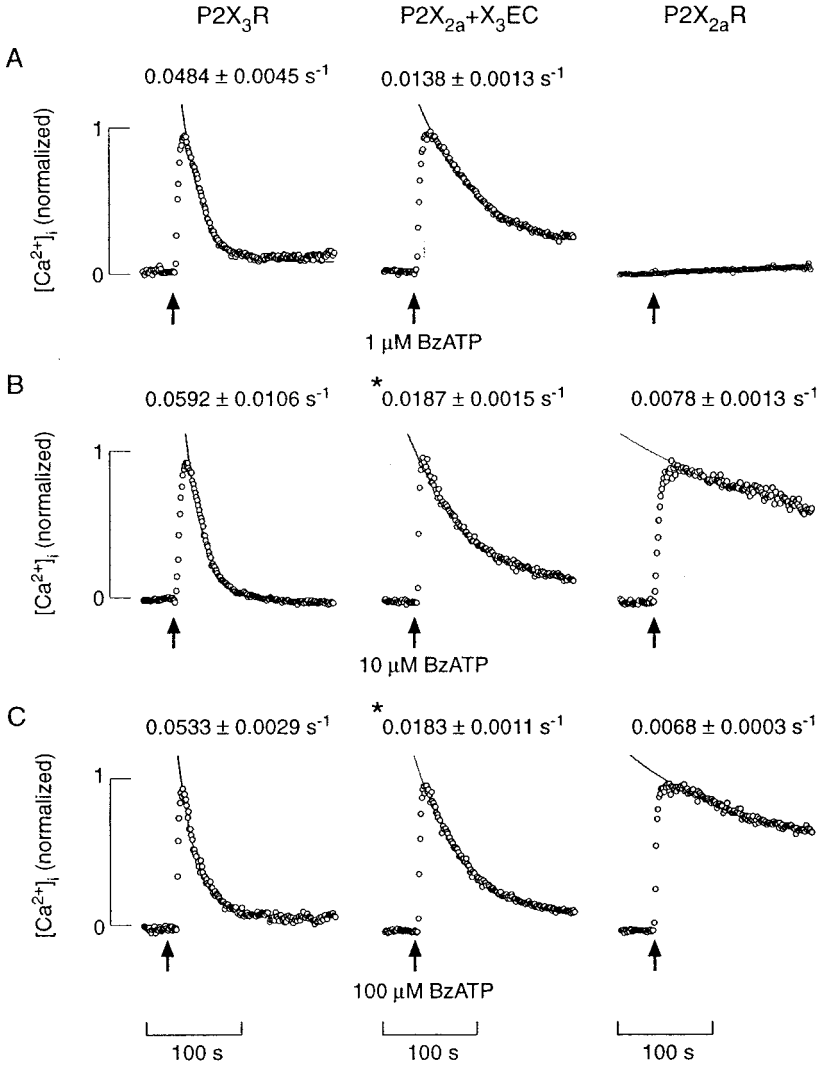

Fig. 7. Patterns of BzATP-induced calcium signaling in GT1 cells expressing wild-type $P2X_3R$ and $P2X_{2a}R$ and chimeric $P2X_{2a}+X_3EC$ receptors. A-C, concentration-dependent effects of BzATP on the rates of calcium signal desensitization in GT1 neurons expressing wild-types and chimeric receptors. Traces shown are representative from three to five independent experiments. Numbers above traces represent mean ± S.E.M. values of desensitization rates. Asterisks indicate significant differences compared with the desensitization rates for $P2X_3R$-and $P2X_{2a}R$-expressing cells.

files (Fig. 9B). In all concentrations studied, ATP was less effective compared with 65 μM BzATP (Fig. 9C), and the estimated EC_{50} was 485 μM (Fig. 9G).

Like $P2X_7R$, chimeric $P2X_{2a}+X_7EC$ and $P2X_{2b}+X_7EC$ receptors showed an inverse sensitivity for BzATP and ATP. The BzATP dose-response curve for chimeric channels was highly similar to that of $P2X_7R$ and was leftward shifted for about half-log concentration compared with the wild-type channels (Fig. 9D). This was accompanied with dramatic increase in the rates of receptor desensitization (Fig. 9E, horizontal arrow). The influence of C-terminal structure on rates and level of receptor desensitization was preserved in chimeric receptors (Fig. 9F).

The chimeric channels showed a rightward shift in the EC_{50} values for ATP, but the agonistic potency of ATP at the chimeric receptor was closer to the ATP potency at wild-type $P2X_2R$ than at wild-type $P2X_7R$ (Fig. 9G). This indicates the relevance of $P2X_2R$ transmembrane domains and/or their flanking Lys^{53}-Ser^{65} and Gly^{311}-Ser^{326} sequences for ATP potency. There was a difference in the rates of $P2X_{2b}+X_7EC$ and $P2X_{2b}R$ desensitization (Fig. 9H, arrow). $P2X_{2a}+X_7EC$ receptors desensitized faster than native $P2X_{2a}R$ (data not shown) and both receptors responded to 500 μM ATP with similar rates of desensitization (Fig. 9I). Table 2 illustrates the lack of C-terminal-specific desensitization for $P2X_2+X_7EC$ receptors when stimulated with ATP. Thus, a small decrease in the agonist potency resulted in a loss of $P2X_2R$ subtype-specific desensitization pattern.

Discussion

Two main hypotheses emerged from previous work on desensitization of P2XRs, one based on the structure of channels, and the other based on the actions of intracellular messengers. The dual control of P2XR may well be expected from studies on such allosteric proteins, and is reminiscent of those seen with other ligand-gated and voltage-gated channels. For example, desensitization of glutamate receptors depends on N-terminal domain (Krupp et al., 1998), the flip-flop cassette (Sommer et al., 1990), and M3–M4 domain (Partin et al., 1995), as well as on intracellular messengers in the postsynaptic cells, including Ca^{2+} (Krupp et al., 1996). The desensitization properties of AMPA receptors can be modified by alternative splicing and mRNA editing, and by heteromeric assembly of channels (Sommer et al., 1990; Robert et al., 2001). In cyclic nucleotide-gated channels, the agonist-binding domain is in the C terminus, and the N-terminal domain alters the efficacy of agonists through in-

teractions with the ligand-binding site by a Ca^{2+}-calmodulin-sensitive mechanism (Tibbs et al., 1997; Varnum and Zagotta, 1997). The structure of intracellular domains of voltage-gated channels are also critical for their voltage-dependent inactivation, whereas the functional control of these channels is mediated by various intracellular messengers (Hille, 1991).

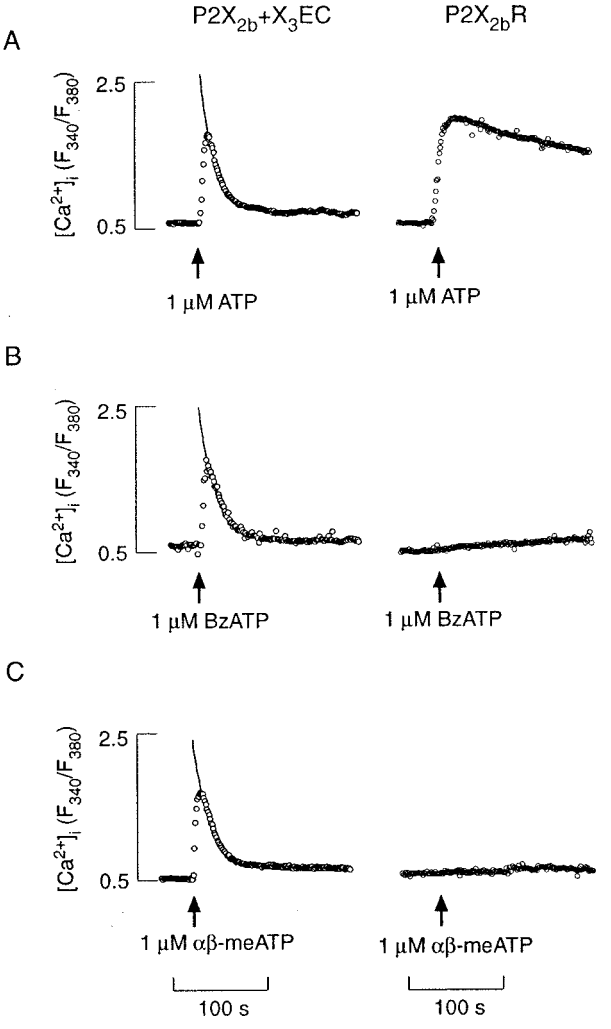

Fig. 8. Agonist-induced calcium signaling in GT1 cells expressing $P2X_{2b}R$ and $P2X_{2b}+X_3EC$ receptors. A to C, typical patterns of $P2X_{2b}R+X_3EC$ desensitization in response to 1 μM ATP (A), 1 μM BzATP (B), and 1 μM $\alpha\beta$-meATP (C). Traces shown are representative from five to six independent experiments. Mean ± S.E.M. values for receptor desensitization kinetics are shown in Table 1.

TABLE 1

The lack of agonist-specific desensitization of chimeric $P2X_{2a}R$ and $P2X_{2b}R$ containing the extracellular domain of $P2X_3Rs$

Data shown are means ± S.E.M. for rates of inactivation of two chimeric receptors. Numbers in brackets indicate number of experiments, each performed in at least 15 cells.

Agonist	$P2X_{2a}+X_3EC$	$P2X_{2b}+X_3EC$
	s^{-1}	
ATP, 1 μM	0.0188 ± 0.0012 (5)	0.0609 ± 0.00696 (8)*
ATP, 10 μM	0.0172 ± 0.0013 (5)	0.0598 ± 0.00375 (5)*
$\alpha\beta$-meATP, 1 μM	0.0193 ± 0.0014 (4)	0.0614 ± 0.0024 (4)*
BzATP, 1 μM	0.0143 ± 0.0011 (7)	0.0660 ± 0.0055 (10)*
BzATP, 10 μM	0.0187 ± 0.0015 (11)	0.0674 ± 0.0079 (7)*
BzATP, 100 μM	0.0183 ± 0.0011 (9)	0.0609 ± 0.0057 (5)*

*, $P < 0.05$.

Here we focused on the mechanism of C-terminal structure-dependent $P2X_2R$ desensitization. Two sister receptors, $P2X_{2a}R$ and $P2X_{2b}R$, exhibit comparable activation profiles for ATP and peak current/$[Ca^{2+}]_i$ responses but desensitize with different rates. $P2X_{2a}Rs$ desensitize slowly and partially, whereas $P2X_{2b}Rs$ desensitize rapidly and to the steady levels significantly lower than that of $P2X_{2a}R$ (Brandle et al., 1997; Simon et al., 1997; Koshimizu et al., 1998b). Similar EC_{50} values for ATP are consistent with identical structure of extracellular domains for these receptors. Different rates of receptor desensitization, on the other hand, indicate the relevance of Val^{370}-Gln^{438} C-terminal sequence, deleted in $P2X_{2b}R$, for receptor-desensitization. In our experiments, potency of several agonists for $P2X_{2a}R$ and $P2X_{2b}R$ were in an order (2-MeS-ATP ≤ ATP ≤ ATPγS < BzATP ≪ $\alpha\beta$-meATP) comparable with results obtained by others (reviewed in Ralevic and Burnstock, 1998).

We also show that these two receptors desensitized in a concentration-dependent manner and with the same order of agonists. However, the IC_{50} values for desensitization were right-shifted compared with the EC_{50} values for activation of channels. This is a novel finding for P2XRs but has been shown for other ligand-gated channels. For example, the extent of AMPA receptor desensitization increases with agonist concentrations (Vyklicky et al., 1991). The half-maximal activation of kainate channels occurs at glutamate concentrations of 330 μM, whereas the half-maximal steady state desensitization occurs at ligand concentrations 20 times lower. A similar ratio was also observed for GluR6 homomers when kainate was used as an agonist (Lerma et al., 2001). Also, concentrations required to desensitize *Torpedo californica* receptors are nearly 1000-fold lower than those required for activation (Corringer et al., 1998). A dual aspect of agonist pharmacology may contribute to the shaping of synaptic currents and modulating the fraction of activatable channels (Jones and Westbrook, 1996). However, the slow and incomplete inactivation of $P2X_{2a}R$ and the right-shifted IC_{50} for ATP argue against such a role of receptor desensitization in neurons expressing these channels.

The receptor subtype-specific desensitization pattern was observed in response to ATP, the native agonist for these channels but also in response to stimulation with two analog agonists, 2-MeS-ATP and ATPγS. However, the receptor-specificity of desensitization was less obvious when stimulated with BzATP and was lost when receptors were stimulated with $\alpha\beta$-meATP. Furthermore, the ligand-specific desensitization patterns were recorded at maximal agonist concentrations, where peak amplitudes in $[Ca^{2+}]_i$ were comparable in $P2X_{2a}R$ and $P2X_{2b}R$. Consistent with a role of agonist-binding domains in desensitization of other ligand-gated channels, both AMPA and glutamate maximally activate AMPA receptors, whereas kainate and domoate act as partial agonists, and produce much less desensitization than glutamate (Patneau and Mayer, 1990; Patneau et al., 1993; Swanson et al., 1997; Armstrong and Gouaux, 2000). The novel aspect in ligand-specific receptor desensitization emerging from this study is in coupling between ectodomain and C-terminal domain. In general, there was a parallelism between the rates of $P2X_{2a}R$ and $P2X_{2b}R$ desensitization and the EC_{50} values for agonists. This suggests that C-terminal-dependent desensitization pattern is not an "all-or-none"

phenomenon but a graded process that probably depends on ligand binding affinity and/or activation efficacy.

The relevance of ectodomain structure on C-terminal-dependent desensitization pattern was further confirmed in experiments with chimeric channels. The agonist-specific desensitization pattern of $P2X_2Rs$ was lost by changing the native binding site of these channels with the $P2X_3R$ extracellular domain. Both chimeras, $P2X_{2a}+X_3EC$ and $P2X_{2b}+X_3EC$, exhibited about 30-, 25-, and 150-fold increase in the EC_{50} values for ATP, BzATP and $\alpha\beta$-meATP, respectively. The rates of desensitization for both chimeric receptors also increased for 2–3-fold. However, the C-terminal structure-dependent desensitization pattern was preserved; like native receptors, $P2X_{2b}+X_3EC$ receptor desensitized more rapidly

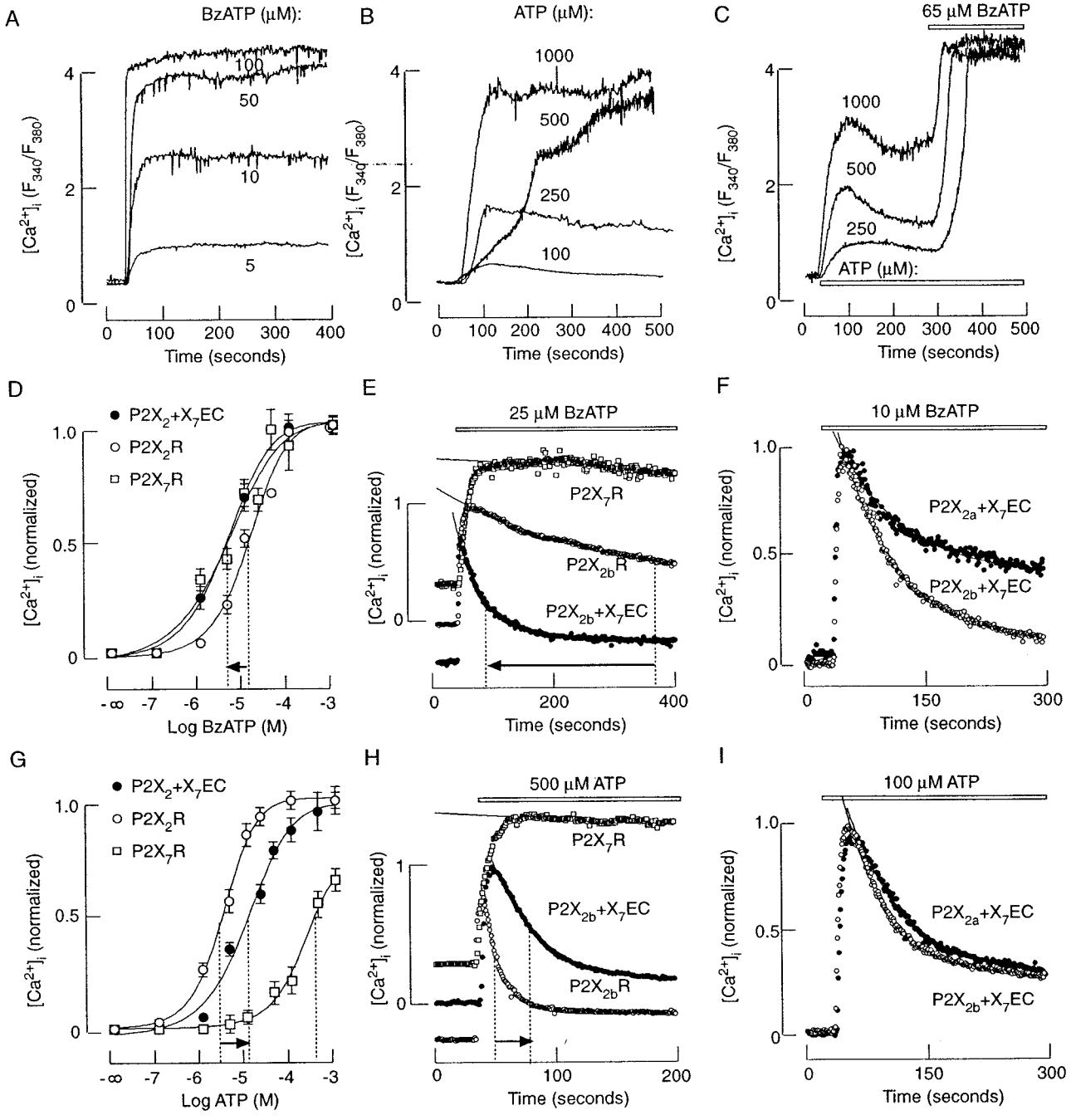

Fig. 9. Characterization of calcium signaling pattern by chimeric $P2X_2Rs$ containing the $P2X_7R$ ectodomain. A to C, characterization of agonist-induced calcium response in $P2X_7R$-expressing cells. Concentration-dependent effects of BzATP (A) and ATP (B) on $[Ca^{2+}]_i$ response. Numbers indicate concentrations of agonists that were continuously present during the recording. C, comparison of the agonistic potency of ATP and BzATP. D to F, comparison of the BzATP effects on peak $[Ca^{2+}]_i$ response (D) and rates of receptor desensitization (E and F) in cells expressing $P2X_2R$, $P2X_7R$, and $P2X_2+X_7EC$ receptors. G to I, comparison of the ATP effects on peak $[Ca^{2+}]_i$ response (G) and rates of receptor desensitization (H and I) in cells expressing $P2X_2R$, $P2X_7R$, and $P2X_2+X_7EC$ receptors. No difference in peak $[Ca^{2+}]_i$ responses were observed between $P2X_{2a}+X_7EC$ and $P2X_{2b}+X_7EC$ and these results are shown combined. Arrows indicate differences in the EC_{50} values (D and G) and half-times for receptor desensitization (E and H). The results shown are means ± S.E.M. with three to eleven experiments per dose. In all, horizontal bars above and below traces indicate the duration of agonist stimulation.

TABLE 2

The lack of C terminus-specific desensitization of chimeric $P2X_{2a}R$ and $P2X_{2b}R$ containing the extracellular domain of $P2X_7Rs$

Data shown are means ± S.E.M. for rates of inactivation of two chimeric receptors. Numbers in brackets indicate number of experiments, each performed in at least 15 cells.

Agonist	$P2X_{2a}+X_7EC$	$P2X_{2b}+X_7EC$
	s^{-1}	
ATP, 100 μM	0.0125 ± 0.0040 (8)	0.0160 ± 0.0007 (6)
ATP, 500 μM	0.0221 ± 0.0016 (4)	0.0242 ± 0.0005 (5)
ATP, 1000 μM	0.0212 ± 0.0015 (4)	0.0259 ± 0.0016 (3)

than $P2X_{2a}+X_3EC$ receptor. Finally, the ligand-specific and receptor subtype-specific desensitization patterns reversed in cells expressing $P2X_{2a}+X_7EC$ and $P2X_{2a}+X_7EC$ receptors. Such chimeras showed lower sensitivity for ATP, compared with native $P2X_2Rs$ and desensitized with comparable rates and higher sensitivity to BzATP accompanied with the C terminus-specific desensitization pattern.

At the present time, it is difficult to discuss the possible molecular mechanism of interactions between the ectodomain and C-terminal domain in development of desensitization. Calcium measurements used in our study provide several advantages. P2XR-generated calcium signals mediate the action of these receptors on cellular functions, including neurotransmission, hormone secretion, transcriptional regulation, and protein synthesis (Berridge, 1993). Thus, calcium rather than current profiles reflect the importance of a particular pattern of signaling on cellular functions. $P2X_2Rs$ conduct calcium and the addition of nifedipine blocks the indirect (through voltage-gated L-type calcium channels) action of activated receptors in our expression system (Koshimizu et al., 2000), reflecting Ca^{2+} influx function of these channels. Single-cell calcium measurements can be done simultaneously in many cells, leading to better statistics, which are critical for interpretation of EC_{50} and rates of desensitization. Measurements of GFP intensities also provide an effective mechanism for selection of cells with comparable expression of P2XRs and more reliable data on peak response and EC_{50} values derived from these experiments (Koshimizu et al., 2000). However, $[Ca^{2+}]_i$ measurements also limit the interpretation of activation and desensitization properties of channels, because of calcium handling mechanism of the cells used in experiments.

Other limitation comes from the fact that the ligand-binding domain structure and the crystal structure of P2XRs have not been identified, in contrast to glutamate channels (Sun et al., 2002). In our chimeric receptors, the extracellular loop is derived almost entirely from $P2X_3R$ and $P2X_7R$. Consistent with this, the ATP potency of the chimeric $P2X_2+X_3EC$ receptors matches the ATP potency at native $P2X_3R$ rather than native $P2X_2R$. However, the ATP potency at the $P2X_2+X_7EC$ receptors is closer to the ATP potency at the parental $P2X_2R$ rather than $P2X_7R$. These contradictory results suggest the relevance of flanking $P2X_2R$ sequences on agonistic potency of ATP. We may speculate that these sequences act as "dominant-positive" domains to offset atypical low sensitivity of $P2X_7R$ for native agonist. In accordance with this view, it has been reported recently that point mutations in the first transmembrane domain, specifically Phe^{44}, affect the ligand-selectivity of rat $P2X_2R$ (Jiang et al., 2001).

In conclusion, our results show that homomeric $P2X_{2a}R$ and $P2X_{2b}R$ exhibit highly comparable EC_{50} values for receptor activation by various agonists, but desensitize in a receptor- and agonist-specific manner. Pharmacological manipulations with activation of these receptors and molecular manipulations with their ectodomains indicate that the efficacy of agonists reflects the ligand-specificity of receptor desensitization; highly potent agonists trigger $P2X_2R$-subtype specific C terminus-mediated desensitization, whereas agonists with lower potency are less effective or ineffective. Thus, it seems that conformational changes needed for activation of $P2X_2Rs$ are not always sufficient to trigger C terminus-controlled desensitization. These findings provide a solid base for further biophysical investigations on hypothesis that the affinity of agonists for receptors determines the strength of molecular conformational changes needed for development of C-terminal-controlled channel desensitization.

References

Armstrong N and Gouaux E (2000) Mechanism for activation and antagonism of an AMPA-sensitive glutamate receptor: crystal structures of the GluR2 ligand binding core. *Neuron* **28:**165–181.

Auerbach A and Akk G (1998) Desensitization of mouse nicotinic acetylcholine receptor-channels. *J Gen Physiol* **112:**181–197.

Berridge MJ (1993) Inositol triphosphate and calcium signaling. *Nature (Lond)* **361:**315–325.

Boue-Grabot E, Archambault V, and Seguela P (2000) A protein kinase C site highly conserved in P2X subunits controls the desensitization kinetics of P2X2 ATP-gated channels. *J Biol Chem* **275:**10190–10195.

Brandle U, Spielmanns P, Osteroth R, Sim J, Surprenant A, Buell G, Ruppersberg JP, Plinkert PK, Zenner HP, and Glowatzki E (1997) Desensitization of the $P2X_2$ receptor controlled by alternative splicing. *FEBS Lett* **404:**294–298.

Chow Y-W and Wang H-L (1998) Functional modulation of P2X2 receptors by cyclic AMP-dependent protein kinase. *J Neurochem* **70:**2606–2612.

Cook SP, Rodland KD, and McCleskey EW (1998) A memory from extracellular Ca^{2+} by speeding recovery of P2X receptors from desensitization. *J Neurosci* **18:**9238–9244.

Corringer P-J, Bertrand S, Bohler S, Edelstein SJ, Changeux J-P, and Bertrand D (1998) Critical elements determining diversity in agonist binding and desensitization of neuronal nicotinic acetylcholine receptors. *J Neurosci* **18:**648–657.

Ding S and Sachs F (2000) Inactivation of P2X2 purinoreceptors by divalent cations. *J Physiol* **522:**199–214.

Ennion SJ and Evans RJ (2002) P2X1 receptor subunit contribution to gating revealed by a dominant negative PKC mutant. *Biochem Biophys Res Commun* **291:**611–616.

Hille B (1991) Ionic channels of excitable membranes. Sinauer Associates Inc., Sunderland, Massachusetts.

Horton RM, Hunt HD, Ho SN, Pullen JK, and Pease LR (1989) Engineering hybrid genes without the use of restriction enzymes: gene splicing by overlap extension. *Gene* **77:**61–68.

Jiang L-H, Rassendern F, Spelta V, Surprenant A, and North RA (2001) Amino acid residues involved in gating identified in the first membrane-spanning domain of the rat P2X2 receptor. *J Biol Chem* **276:**14902–14908.

Jones MV and Westbrook GL (1996) The impact of receptor desensitization on fast synaptic transmission. *Trends Neurosci* **19:**96–101.

Koshimizu T, Koshimizu M, and Stojilkovic S (1999) Contributions of the C-terminal domain to the control of P2X receptor desensitization. *J Biol Chem* **274:**37651–37657.

Koshimizu T, Tomic M, Koshimizu M, and Stojilkovic SS (1998a) Identification of amino acid residues contributing to desensitization of the $P2X_2$ receptor channel. *J Biol Chem* **273:**12853–12857.

Koshimizu T, Tomic M, Van Goor F, and Stojilkovic SS (1998b) Functional role of alternative splicing in pituitary $P2X_2$ receptor-channel activation and desensitization. *Mol Endocrinol* **12:**901–913.

Koshimizu T, Van Goor F, Tomic M, Wong AOL, Tanoue A, Tsujimoto G, and Stojilkovic SS (2000) Characterization of calcium signaling by purinergic receptor-channels expressed in excitable cells. *Mol Pharmacol* **58:**936–945.

Krupp JJ, Vissel B, Heinemann SF, and Westbrook GL (1996) Calcium-dependent inactivation of recombinant *N*-methyl-D-aspartate receptors is NR2 subunit specific. *Mol Pharmacol* **50:**1680–1688.

Krupp JJ, Vissel B, Heinemann SF, and Westbrook GL (1998) N-terminal domains in the NR2 subunit control desensitization of NMDA receptors. *Neuron* **20:**317–327.

Lerma J, Paternain AV, Rodriguez-Moreno A, and Lopez-Garcia JC (2001) Molecular physiology of kainate receptors. *Physiol Rev* **81:**971–998.

Lewis C, Neidhart S, Holy C, North RA, Buell G, and Surprenant A (1995) Coexpression of $P2X_2$ and $P2X_3$ receptor subunits can account for ATP-gated currents in sensory neurons. *Nature (Lond)* **377:**432–435.

McBain CJ and Mayer ML (1994) *N*-methyl-D-aspartic acid receptor structure and function. *Physiol Rev* **74:**723–760.

North RA and Barnard EA (1997) Nucleotide receptors. *Curr Opin Neurobiol* **7:**346–357.

Partin KM, Bowie D, and Mayer ML (1995) Structural determinants of allosteric regulation in alternatively spliced AMPA receptors. *Neuron* **14:**833–843.
Patneau DK and Mayer ML (1990) Structure-activity-relationship for amino-acid transmitter candidates acting at *N*-methyl-D-aspartate and quisqualate receptors. *J Neurosci* **10:**2385–2399.
Patneau DK, Vyklicky L, and Mayer ML (1993) Hippocampal neurons exhibit cyclothiazide-sensitive rapidly desensitizing responses to kainate. *J Neurosci* **13:** 3496–3509.
Paukert M, Oseroth R, Geisler H-S, Brandle U, Glowatzki E, Ruppersberg JP, and Grunder S (2001) Inflammatory mediators potentiate ATP-gated channels through the P2X3 subunit. *J Biol Chem* **276:**21077–21082.
Radford KM, Virginio C, Surprenant A, North A, and Kawashima E (1997) Baculovirus expression provides direct evidence for heteromeric assembly of $P2X_2$ and $P2X_3$ receptors. *J Neurosci* **17:**6529–6533.
Ralevic V and Burnstock G (1998) Receptors for purines and pyrimidines. *Pharmacol Rev* **50:**413–492.
Robert A, Irizarry SN, Hughes TE, and Howe JR (2001) Subunit interactions and AMPA receptor desensitization. *J Neurosci* **21:**5574–5586.
Simon J, Kidd EJ, Smith FM, Chessell IP, Murrell-Lagnado R, Humphrey PPA, and Barnard EA (1997) Localization and functional expression of splice variants of the $P2X_2$ receptor. *Mol Pharmacol* **52:**237–248.
Smith FM, Humphrey PPA, and Murrell-Lagnado RD (1999) Identification of amino acids within the P2X2 receptor C terminus that regulate desensitization. *J Physiol* **520:**91–99.
Sommer B, Keinanen K, Verdoorn TA, Wisden W, Burnashev N, Herb A, Kohler M, Takagi T, Sakmann B, and Seeburg PH (1990) Flip and flop—a cell-specific functional switch in glutamate-operated channels of the CNS. *Science (Wash DC)* **249:**1580–1585.
Sun Y, Olson R, Horning M, Armstrong N, Mayer M, and Gouaux E (2002) Mechanism of glutamate receptor desensitization. *Nature (Lond)* **417:**245–253.
Surprenant A, Rassendren F, Kawashima E, North RA, and Buell G (1996) The cytosolic P_{2Z} receptor for extracellular ATP identified as a P_{2X} receptor ($P2X_7$). *Science (Wash DC)* **272:**735–738.
Swanson GT, Kamboj SK, and Cull-Candy SG (1997) Single channel properties of recombinant AMPA receptors depend on RNA editing, splice variations and subunit composition. *J Neurosci* **17:**58–69.
Tibbs GR, Goulding EH, and Siegelbaum SA (1997) Allosteric activation and tuning of ligand efficacy in cyclic-nucleotide-gated channels. *Nature (Lond)* **386:**612–615.
Varnum MD and Zagotta WN (1997) Interdominant interactions underlying activation of cyclic nucleotide-gated channels. *Science (Wash DC)* **278:**110–113.
Vyklicky L, Patneau DK, and Mayer ML (1991) Modulation of excitatory synaptic transmission by drugs that reduce desensitization at AMPA kainate receptors. *Neuron* **7:**971–984.
Werner P, Seward EP, Buell GN, and North RA (1996) Domains of P2X receptors involved in desensitization. *Proc Natl Acad Sci USA* **93:**15485–15490.
Zhou Z, Monsma LR, and Hume RI (1998) Identification of a site that modifies desensitization of $P2X_2$ receptors. *Biochem Biophys Res Commun* **252:**541–545.

Address correspondence to: Dr. Stanko Stojilkovic, SCS/ERRB/NICHD, Bldg. 49, Room 6A-36, 49 Convent Drive, Bethesda, MD 20892-4510. E-mail: stankos@helix.nih.gov